文章编号： 1007-8827(2019)04-0367-06

CO_2 活化对聚硅氧烷裂解 SiC 衍生炭孔结构的影响

段力群[1]， 马青松[2]， 马林建[1]， 董 璐[1]， 王 波[1]， 代晓青[1]， 张 波[1]
(1. 陆军工程大学 爆炸冲击防灾减灾国家重点实验室，江苏 南京 210007；
2. 国防科技大学 新型陶瓷纤维及其复合材料国防科技重点实验室，湖南 长沙 410073)

摘 要： 经聚硅氧烷裂解转化得到碳化硅粉体，然后对其进行氯化处理得到炭，再通过 CO_2 活化处理得到具有高比表面积(1 316.8 ~ 1 929.0 $m^2 \cdot g^{-1}$)的微孔炭(SiC-DC)材料。研究了 CO_2 活化温度、时间对 SiC 衍生多孔炭结构的影响。采用氮气吸附法、X-ray 衍射光谱(XRD)、扫描电镜(SEM)及透射电镜(TEM)等技术对 SiC-DC 样品微观结构随活化温度、时间演变进行表征分析。结果表明，CO_2 活化处理可以有效调控 SiC-DC 的孔结构，而对其结晶性影响很小，且活化处理后样品保持着 SiC 粉体或未活化 SiC-DC 样品的原有形态和微观结构(如石墨带)。对于已活化 SiC-DC 样品，比表面积(SSA)、总孔容(V_{tot})及微孔孔容都随活化温度、时间增加而增加，但同时活化产率逐渐降低。相比未活化样品，SiC-DC 在 950 ℃条件下活化处理 2 h 后，SSA 和 V_{tot} 值分别增加了 46.5%、86.4%，主要原因是经活化处理，微孔孔容明显增加。

关键词： 聚硅氧烷；碳化硅；碳化硅衍生碳；孔结构；CO_2 活化
中图分类号： TQ127.1+1 **文献标识码：** A

基金项目：江苏省自然科学基金(BK20170754).
通讯作者：马青松，研究员. E-mail：nudtmqs1975@163.com
作者简介：段力群，博士. E-mail：850082427@qq.com

Effect of the CO_2 activation parameters on the pore structure of silicon carbide-derived carbons

DUAN Li-qun[1], MA Qing-song[2], MA Lin-jian[1], DONG Lu[1],
WANG Bo[1], DAI Xiao-qing[1], ZHANG Bo[1]
(1. *State Key Laboratory of Disaster Prevention & Mitigation of Explosion & Impact, Army Engineering University of PLA, Nanjing* 210007, *China*;
2. *Science and Technology on Advanced Ceramic Fibers &Composites Laboratory, National University of Defense Technology, Changsha* 410073, *China*)

Abstract: A silicon carbide derived carbon (SiC-DC) with a high specific surface area (SSA) fabricated by chlorination of a silicon carbide derived from polysiloxane was activated by CO_2. The effect of activation temperature and time on the microstructure of the activated samples was investigated by N_2 sorption, XRD, SEM and TEM. Results showed that CO_2 activation effectively changed the pore structure of the SiC-DC and had little impact on carbon crystallinity. The activated samples retained the morphology of the SiC powder or the non-activated SiC-DC. The SSA, total pore volume (V tot) and micropore volume of the activated SiC-DCs all increased and the yield decreased with increasing activation temperature or time. The SSA and Vtot increased by 46.5 % (from 1 316.8 to 1 929.0 $m^2 \cdot g^{-1}$) and 86.4 % (from 0.560 to 1.044 $cm^3 \cdot g^{-1}$), respectively after the SiC-DC was activated at 950 ℃ for 2 h, mainly as a result of the increased micropore volume.

Key words: Polysiloxane; Silicon carbide; Carbide derived carbon; Pore structure; CO_2 activation

Received date: 2019-04-29; Revised date: 2019-06-30
Foundation item: Natural Foundation of Jiangsu Province, China(BK20170754).
Corresponding author: MA Qing-song, Professor. E-mail: nudtmqs1975@163.com
Author introduction: DUAN Li-qun, Ph. D. E-mail: 80082427@qq.com
English edition available online ScienceDirect (http://www.sciencedirect.com/science/journal/18725805).
DOI: 10.1016/S1872-5805(19)60019-3

1 Introduction

Carbide derived carbons (CDCs) have been attracting much attention in recent years for their high efficiency in a large number of applications such as hydrogen and methane storage[1-3], electrode material in supercapacitors[4-6] or Li-ion batteries[7], protein sorbents[8,9] and for tribological films[10,11]. By choosing a carbide precursor, chlorination temperature and annealing procedure, the pore structures and proper-

ties of nanoporous CDCs can be finely controlled. Nevertheless, their specific surface areas or pore volumes were limited by the atom ratio of M/C in carbide precursors (M_xC_y). Consequently, activation techniques, which are often used for fabrication of nanoporous carbon materials, can be applied to CDCs. Related studies have been reported in ref. [12-15].

Among all conventional activation techniques, physical activation by CO_2 is often used for the reason that CO_2 is a relatively mild oxidizer, which leads to a better control over the development of microporosity during activation as compared with other reagents such as oxygen, steam and air[16,17]. Its low cost and simple manipulation is also attractive to researches. However, it's not easy to find optimal conditions to balance the carbon yield and desired porosity. Besides, their optimal conditions may also vary with different CDCs and applications.

In this paper, we fabricated a kind of microporous silicon carbide derived carbons (SiC-DCs) from polysiloxane, and the effect of activation temperature and time on their pore structure was investigated. The carbon crystallinity under different conditions was also studied simultaneously.

2 Experimental

2.1 Sample preparation

SiC ceramics were produced from commercially available polymethyl (phenyl) siloxane resin (Dow Corning 249 flake resin). The polysiloxane precursor was firstly cross-linked at 250 ℃ in air for 4 h, and crushed into powders by using a disintegrator. The powder (with particle sizes ranging from 150-250 μm) was placed in a graphite crucible and heated to 1 200 ℃ for 2 h under nitrogen (99.999% pure) with a heating rate of 5 ℃/min and then allowed to cool naturally. Subsequently, the SiOC was ball-milled to micron powders (<20 μm particle size) and thermal-treated at 1 700 ℃ under vacuum for 6 h.

The SiC powder was placed in a horizontal tube furnace (diameter 60 mm), purged with nitrogen, heated to 900 ℃ with a rate of 5 ℃ · min^{-1} and exposed to dry chlorine gas (15-20 $cm^3 \cdot min^{-1}$) for 3 h. After chlorination, the sample was treated at 600 ℃ for 2 h under flowing ammonia (NH_3) in order to remove residual chlorine and volatile chlorides trapped in pores. As-prepared SiC-DC sample was treated in the same horizontal tube furnace under flowing CO_2 atmosphere (15-20 $cm^3 \cdot min^{-1}$) at different temperatures with different dwelling times.

2.2 Characterization

Quantitative elemental analysis (EA) of the samples was performed on a LECOCS600 for carbon in the SiC ceramics (Table 1). The perchloric acid dehydration gravimetric method was adopted for the determination of Si content. And the residue element is considered to be oxygen. Given that the carbon atoms should connect with each other or Si atoms while O atoms connect with Si atoms only, atomic formula and calculated composition could be obtained according to ref. [18]. It is calculated that nearly 3.66 wt.% of the as-prepared SiC ceramics from PSO is assigned to free carbon, and the atom ratio of C/Si (C versus Si atoms) reached 1.13. The amount of oxygen atoms can be neglected.

Table 1 Elemental composition of SiC powders.

Composition /wt.%			Atomic formula	Calculated composition	Free carbon /wt.%
Si	O	C			
67.44	-	32.56	$SiC_{1.13}$	$SiC_{1.00}+C_{0.13}$	3.66

Note: Atomic formula is based on the formula SiO_xC_y[18]. Calculated composition is based on the formula $SiO_xC_{(1-x/2)} + y\text{-}(1\text{-}x/2)C_f$[18].

N_2 adsorption-desorption isotherms were obtained using a Quantachrome instrument at 77 K. The Brunauer-Emmertt-Teller (BET) method was used to determine the specific surface area (SSA). The quenched solid density functional theory (QSDFT) was used to analyze the pore size distributions (PSDs) and pore volumes. Scanning electron microscopy (SEM) was performed on the samples with no sputter coating using a HITACHI FEG S4800 scanning electron microscope operating at 10 kV. The samples for transmission electron microscopy (TEM) were prepared by dispersing powders in ethanol and dropping the solutions over a copper grid. TEM measurements were performed using a JEOL JEM2100F microscope operating at 200 kV. X-ray diffraction (XRD) analysis was managed using a Rigaku diffractometer with Cu $K\alpha$ radiation ($k = 0.154$ nm) operated at 30 mA and 40 kV. XRD patterns were collected using step scans, with a step size of 0.01° (2θ) and a count time of 2 s per step between 10° (2θ) and 80° (2θ).

3 Results and discussion

To investigate the effect of CO_2 activation conditions on the pore structure of SiC-DCs, two factors (activation temperature and time) were considered in this paper. Table 2 summarizes the weight loss of the

non-activated sample (SiC-DC) as a function of activation temperature and time. We could observe that the values of weight loss increased with increasing activation temperature and time. It's worth noting that the value of weight loss was very small (0.3 wt. %) when the SiC-DC was activated at 750 ℃ for 2 h, implying that a higher temperature should be needed. However, when the activation was carried out at 1 000 ℃ for 2 h or at 950 ℃ for 3 h, a high weight loss (beyond 75 wt. %) was observed. Therefore, it can be concluded that the suitable CO_2 activation for this material should be carried out at 800-950 ℃ for 1-3 h.

Table 2　Weight loss of SiC-DC as a function of activation condition.

Temperature /℃	Time /h	Weight loss /wt. %
750	2	0.3
800	2	8
850	2	20
900	2	31
950	2	55
1000	2	82
900	1	26
900	3	42
950	3	75

3.1　Activation temperature

Fig. 1 shows the N_2 adsorption-desorption isotherms and the corresponding pore size distributions of samples activated at different temperatures. All samples exhibit a type I isotherm (Fig. 1a) according to the IUPAC classification[19], suggesting that the samples were predominantly microporous. No obvious hysteresis loop was observed for all samples after activation, meaning that the samples own few mesopores. Besides, the curves show some tiny tails at high relatively pressures ($p/p_0>0.9$), implying that a few macropores also exist in these samples. Furthermore, it can be observed the isotherm curves uplift with increasing activation temperature. This change is consistent with the weight loss evolution caused by activation. Then, we can infer that increasing activation temperature is helpful for generating micropores.

The corresponding pore size distributions (PSDs) of samples activated at different temperatures are calculated by the quenched solid density functional theory (QSDFT), as shown in Fig. 1b. All samples exhibit a single narrow peak at about 0.9 nm. And it is found that the peak moves toward the right direction and becomes high with increasing the activation temperature, indicating that a higher temperature activation will lead to a larger size and a higher number of micropores. Besides, when the temperature reached up to 950 ℃, a tiny should-peak centered at ~2 nm was observed. This phenomenon indicated a transition from micropores to mesopores to some extent.

Pore parameters are summarized in Table 3. We can see the specific surface area (SSA) and total pore volume (V_{tot}) of SiC powders are very small, implying that very few pores exist in this SiC powders. For the carbon samples, the value of SSA and V_{tot} both increase with the activation temperature, with maximum values of 1 929 $m^2 \cdot g^{-1}$ and 1.044 $cm^3 \cdot g^{-1}$, respectively. Actually, the value for SSA increases by 46.5% for the sample activated at 950 ℃ for 2 h as compared with the non-activated sample. This change is mainly contributed by the augment of micropore volume (V_{mic}). The ratio of micropore volume to total pore volume (V_{mic}/V_{tot}) is very high (beyond 85%), demonstrating that CO_2 activation prefers to increase micropores under the studied conditions.

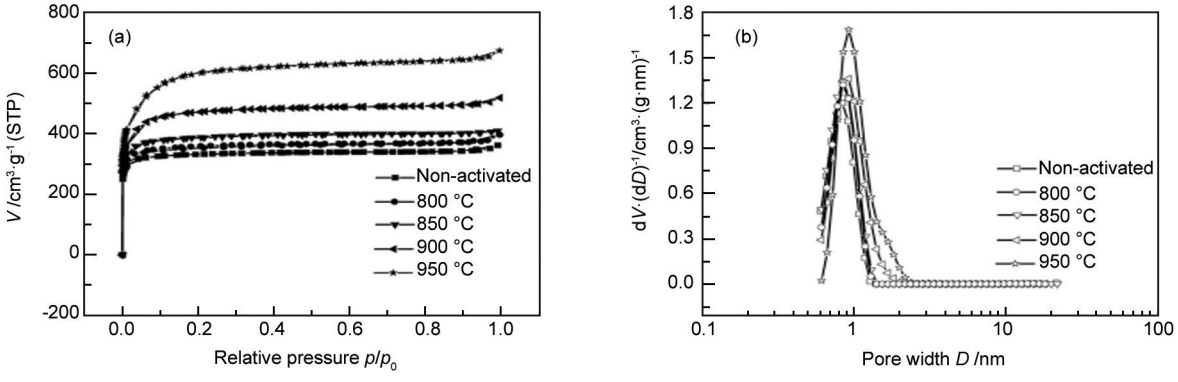

Fig. 1　(a) N_2 sorption isotherms and (b) corresponding pore size distributions for SiC-DC samples activated at different temperatures for 2 h.

Table 3 Summary of pore parameters for SiC powders and SiC-DC samples activated under different conditions.

Sample		SSA	V_{tot}	V_{mic} ($d \leqslant 2$ nm)	V_{mic}/V_{tot}
Temperature /℃	Time /h	/$m^2 \cdot g^{-1}$	/$cm^3 \cdot g^{-1}$	/$cm^3 \cdot g^{-1}$	/%
SiC powders		4.3	0.012	-	-
Non-activated SiC-DC		1316.8	0.560	0.487	87
800	2	1404.2	0.617	0.523	85
850	2	1502.6	0.636	0.571	90
900	2	1814.8	0.806	0.705	87
950	2	1929.0	1.044	0.896	85
900	1	1491.3	0.687	0.564	82
900	3	1903.7	0.951	0.806	85

Note: Specific surface area (*SSA*) estimated at $p/p_0 = 0.05$-0.25. V_{tot}—total pore volume, calculated at $p/p_0 = 0.99$. V_{mic}—Calculated by quenched solid density functional theory (QSDFT) method using equilibrium model for slit pores. '-' symbols a small value which is close to zero.

The carbon crystallinity evolution of the samples as a function of activation temperature is determined by X-ray diffractions (XRD) as shown in Fig. 2. The SiC powder showed a typical diffraction pattern of β-SiC (or moissanite-3C with a cubic structure), characterized by broad diffraction peaks at 35.6°, 41.4°, 60°, 71.8°, 75.5° (2θ), corresponding to (111), (200), (220), (311) and (222) SiC phases, respectively. For other samples, two broad peaks centered at ~26° and ~44° were observed, which were designated to a typical characteristic of amorphous carbon. Besides, the discrepancy between these images could nearly be neglected for all samples, suggesting there is no obvious difference of carbon crystallinity of the samples by CO_2 activation.

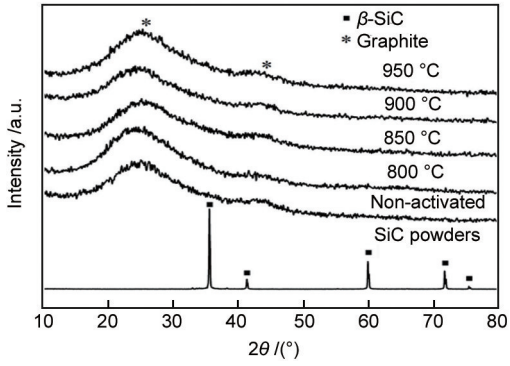

Fig. 2 XRD patterns of SiC powders and SiC-DC samples activated at different temperatures for 2 h.

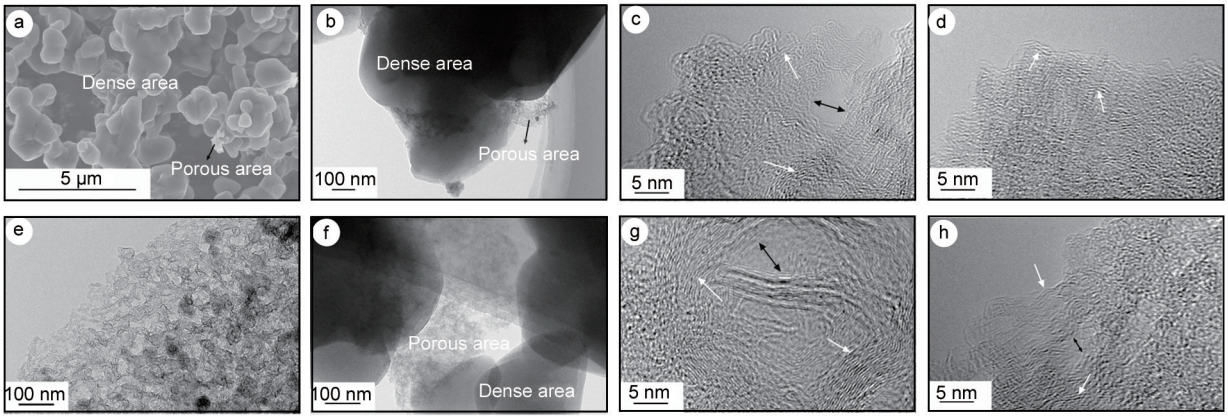

Fig. 3 (a) SEM image and (b-h) TEM images of the SiC-DC samples.
(a-d: Non-activated sample; e-h: The sample treated by CO_2 activation at 900 ℃ for 2 h. White arrow symbols graphite ribbons, and black double arrows symbol nanopores. (c-h) TEM images are attributed to porous area and dense area of two samples above, respectively.)

Fig. 3 depicts SEM and TEM images of the non-activated sample and the sample activated at 900 ℃ for 2 h. Since the carbon crystallinity has a small change as a function of the activation temperature, images for the other activated samples are not shown here. It can be observed that both two samples have a dominant dense area and a small proportion of porous area. And the amorphous structure and graphite ribbons are observed on both the dense and porous areas. This phenomena are well in accord with the microscopic morphology of the SiC powders pyrolyzed from polysiloxane, as shown in Fig. 4. Graphite ribbons can be easily found in the edges of crystalline SiC particles, especially in the porous area. According to literatures[20,21] and our previous work[22], SiOC experiences a carbothermal reaction (SiO_2 + 3C

→ SiC + 2CO). The silica phase is yielded by the phase separation as $SiC_xO_{2(1-x)} \rightarrow xSiC + (1-x)SiO_2$. Abundant nanopores can be generated during the carbothermal reaction. Nevertheless, most pores will disappear again due to partial sintering of the nanocrystalline SiC and viscous flow of silica at a high temperature[23,24]. Simultaneously, the free carbon in SiOC experiences a transition from an amorphous structure to graphite, and a small part may be derived from the SiC framework ($SiC_x \rightarrow SiC + (x-1)C$). Thus, a small area of the samples seems in a high porosity (Fig. 3). However, it is worth noting that for the SiC-DC and its activated products, there are relatively abundant and homogeneous microporous pores in both the dense and porous areas, which is different from the SiC powder. The graphite ribbons were demonstrated to be the free carbon in the SiC ceramics from polysiloxane[25]. Obviously, the activated samples preserved the previous morphology and microstructures (like graphite ribbons) of SiC ceramics and the non-activated sample.

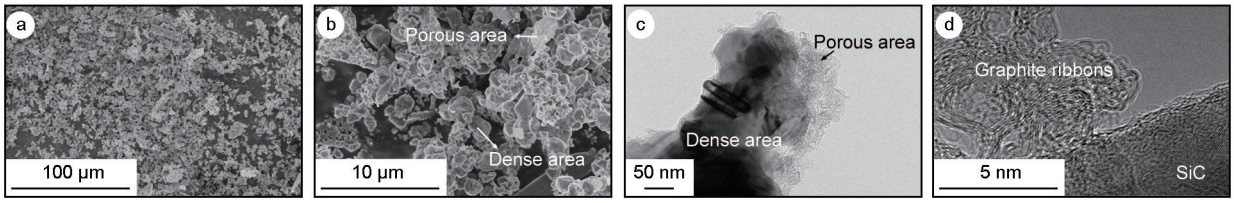

Fig. 4　(a,b) SEM and (c,d) TEM images of the SiC powders.

3.2　Activation time

From the results above, we can infer that the pore structure of the SiC-DC will be subjected to an obvious change at the activation temperature of 900 ℃. Thus, the effect of activation time on the pore structure of the SiC-DC was further investigated at this temperature. Fig. 5 shows the N_2 adsorption-desorption isotherms and the corresponding pore size distributions of the samples activated at 900 ℃ for different times. For all samples, the isotherms (Fig. 5a) can be classified as a type I, which indicates that carbon materials are microporous after activation. Besides, it can be found that the curves uplift with increasing the activation time. The corresponding pore size distributions (PSDs) of the samples activated for different times are shown in Fig. 5b. Obviously, the PSDs are single-modal and narrow, with the range of 0.6-2 nm. Furthermore, the pore peak moves toward the right direction and becomes high with increasing the activation time, meaning that a longer activation time will also lead to an increase of the size and the numbers of micropores. These phenomena are very similar to the results above at different activation temperatures.

Pore parameters for the samples activated at 900 ℃ for different times are also summarized in Table 3. We can see that the SSA of the SiC-DC increased mildly. When the as-received sample was activated for 2 h, the SSA and V_{tot} increased by 37.8% and 43.9%, reaching up to 1 814.8 $m^2 \cdot g^{-1}$ and 0.806 $cm^3 \cdot g^{-1}$, respectively. As the activation time was extended further to 3 h, the SSA and V_{tot} uplift by 44.6% and 68.9%, respectively. Therefore, it can be inferred that the V_{tot} increases faster than the SSA when the activation time is beyond 2 h. This change might be explained by the reason that the pore size would be enlarged when a long activation time was adopted.

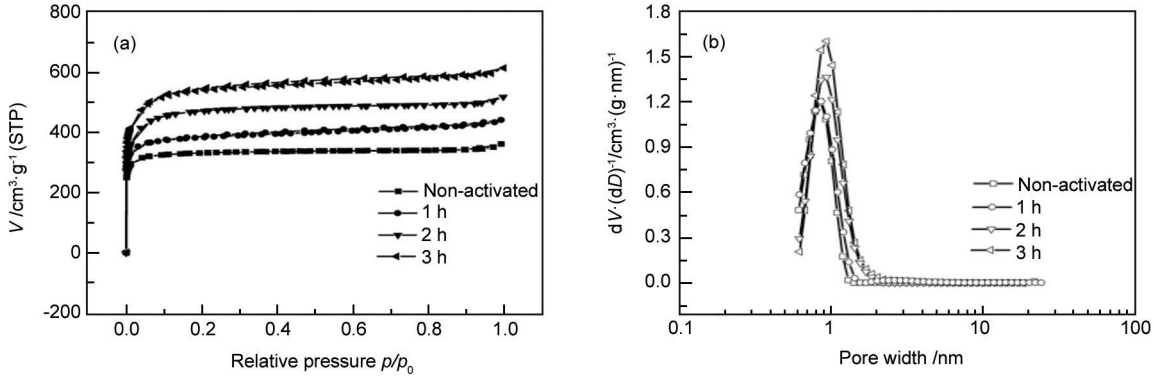

Fig. 5　(a) N_2 sorption isotherms and (b) corresponding pore size distributions for SiC-DC samples activated at 900 ℃ with different times.

4 Conclusions

CO_2 activation could further improve the porosity of SiC-DCs. Interestingly, this method prefers to increase the microporosity other than meso- or macroporosity, and has little impact on carbon crystallinity. The maximum SSA (1 929 $m^2 \cdot g^{-1}$) was obtained at 950 ℃ for 2 h. Nevertheless, the transition from microporosity to mesoprosity will happen when a high activation temperature (beyond 850 ℃ for 2 h) or a long activation time (beyond 2 h at 900 ℃) is employed.

References

[1] Vakifahmetoglu C, Presser V, Yeon S H, et al. Enhanced hydrogen and methane gas storage of silicon oxycarbide derived carbon[J]. Microporous Mesoporous Mater, 2011, 144: 105-112.

[2] Gogotsi Y, Dash R K, Yushin G, et al. Tailoring of nanoscale porosity in carbide-derived carbons for hydrogen storage[J]. J Amer Chem Soc, 2005, 127: 16006-16007.

[3] Yushin G, Dash R, Jagiello J, et al. Carbide-derived carbons: Effect of pore size on hydrogen uptake and heat of adsorption [J]. Adv Funct Mater, 2006, 16: 2288-2293.

[4] Li Y F, Liu Y Z, Liang Y, et al. Preparation of nitrogen-doped graphene/activated carbon composite papers to enhance energy storage in supercapacitors[J]. Appl. Phys. A, 2017, 123: 566.

[5] Sun G, Song W, Liu X, et al. New concept of in situ carbide-derived carbon/xerogel nanocomposite materials for electrochemical capacitor[J]. Mater Lett, 2011, 65: 1392-1395.

[6] Wei F, Zhang H F, He X J, et al. Synthesis of porous carbons from coal tar pitch for high-performance supercapacitors [J]. New Carbon Materials, 2019, 34(2): 132-139.

[7] Kotina I M, Lebedev V M, Ilves A G, et al. Study of the lithium diffusion in nanoporous carbon materials produced from carbides[J]. J Non-Crystal Solids, 2002, 299/302: 815-819.

[8] Yushin G, Hoffmana E N, Barsoum M W, et al. Mesoporous carbide-derived carbon with porosity tuned for efficient adsorption of cytokines[J]. Biomaterials, 2006, 27: 5755-5762.

[9] Yachamaneni S, Yushin G, Yeon S H, et al. Mesoporous carbide-derived carbon for cytokine removal from blood plasma[J]. Biomaterials, 2010, 31: 4789-4794.

[10] McNallan M, Ersoy D, Zhu R, et al. Nano-structured carbide-derived carbon films and their tribology [J]. Tsinghua Sci Technol, 2005, 10(6): 699-703.

[11] Erdemir A, Kovalchenko A, McNallan M J, et al. Effects of high-temperature hydrogenation treatment on sliding friction and wear behavior of carbide-derived carbon films[J]. Surf Coat Technol, 2004, 188: 588-593.

[12] Schmirler M, Glenk F, Etzold B J M. In-situ thermal activation of carbide-derived carbon[J]. Carbon, 2011, 49: 3679-3686.

[13] Gogotsi Y, Portet C, Osswald S, et al. Importance of pore size in high-pressure hydrogen storage by porous carbons[J]. Int J hydrogen energy, 2009, 34: 6314-6319.

[14] Yeon S H, Osswald S, Gogotsi Y, et al. Enhanced methane storage of chemically and physically activated carbide-derived carbon[J]. J Power Sources, 2009, 191: 560-567.

[15] Osswald S, Portet C, Gogotsi Y, et al. Porosity control in nanoporous carbide-derived carbon by oxidation in air and carbon dioxide[J]. J Solid State Chem, 2009, 182: 1733-1741.

[16] Xia K, Gao Q, Song S, et al. CO_2 activation of ordered porous carbon CMK-1 for hydrogen storage[J]. Int J hydrogen energy, 2008, 33: 116-123.

[17] Yusof N, Ismail A F, Rana D, et al. Effects of the activation temperature on the polyacrylonitrile/acrylamide-based activated carbon fibers[J]. Mater Lett, 2012, 82: 16-18.

[18] Belot V, Corriu R J P, Leclercq D, et al. Silicon oxycarbide glasses with low O/Si ratio from organosilicon precursors[J]. J. Non-Crystalline Solids. 1994, 176: 33-44.

[19] Sing K S W, Everett D H, Haul R A W, et al. Reporting physisorption data for gas/solid systems[J]. Pure Appl Chem, 1985, 57 (4): 603-619.

[20] Kleebe H J, Blum Y D. SiOC ceramic with high excess free carbon[J]. J Eur Ceram Soc, 2008, 28: 1037-1042.

[21] Xu T, Ma Q, Chen Z. The effect of environment pressure on high temperature stability of silicon oxycarbide glasses derived from polysiloxane[J]. Mater Lett, 2011, 65: 1538-1541.

[22] Duan L, Ma Q. Effect of pyrolysis temperature on the pore structure evolution of polysiloxane-derived ceramics[J]. Ceram Int, 2012, 38: 2667-2671.

[23] Fukushima M, Zhou Y, Yoshizawa Y I. Fabrication and microstructural characterization of porous silicon carbide with nanosized powders[J]. Mater Sci Eng B, 2008, 148: 211-214.

[24] Ma Q, Ma Y, Chen Z. Fabrication and characterization of nanoporous SiO_2 ceramics via pyrolysis of silicone resin filled with nanometer SiO_2 powders [J]. Ceram Int, 2010, 36: 2269-2272.

[25] Duan L, Ma Q, Chen Z. Fabrication and CO_2 capture performance of silicon carbide derived carbons from polysiloxane[J]. Microporous Mesoporous Mater, 2015, 203: 24-31.